 <b>G E C A L S T H O M</b> POWER GENERATION	TECHNICAL SUBMISSION TO SOUTHERN CALIFORNIA EDISON SUBMISSION No.3		
	Large Steam Turbines Mech. Analysis Group	Engineer: J. Bolton Date 14th October 1997	Page 1 of 62
Title: <b>SAN ONOFRE RETROFIT MISSILE ANALYSIS REPORT</b> Rev. 1*			

**Summary**

This report presents the assessment of possible mechanisms of fracture of the new LP rotors to be retrofitted into the turbine units at San Onofre. The probability of failures occurring is shown to be very low and to be in compliance with USNRC safety regulations, based on an interval of 10 years between rotor inspections. The masses and energies of potential missiles are presented and shown to be lower than for the original units.

**List of Contents**

- i. Introduction
2. Probability of rotor fracture
  - 2.1 Mechanisms of rotor fracture
  - 2.2 Probability of attaining specific turbine overspeeds
  - 2.3 Probability of LP rotor failure at specific overspeeds
    - 2.3.1 Failure at runaway
    - 2.3.2 Failure at speeds below runaway
      - 2.3.2.1 Failure due to fatigue
      - 2.3.2.2 Failure due to stress corrosion
  - 2.4 Overall probabilities of failure
3. Turbine missile characteristics
  - 3.1 Mechanism of disintegration
  - 3.2 Size of missiles
  - 3.3 Energy lost in casing penetration
4. Probability of generating external missiles

\* EDITED VERSION - PROPRIETARY INFORMATION REMOVED

Newbold Road, Rugby, Warwickshire, England, CV21 2NH  
 Telephone: 01788 577111 Telex: 84023430 GATE G Fax: 01788 531700

GEC ALSTHOM Turbine Generators Limited  
 Registered Office: Newbold Road, Rugby, Warwickshire. Registered in England No. 561851

9810300304 981029  
 PDR ADOCK 05000361  
 P PDR

18TDJB76

### List of Appendices

1. Overspeed analysis
2. Influence of test intervals on failure probability
3. Probability of bursting at runaway overspeed
4. Reference sources

### List of Tables

1. Calculated bursting speeds
2. Fatigue crack growth calculations
3. SCC margins for new rotors
4. Illustrative trial calculations for SCC cracks
5. Conditional probability of failure by SCC
6. Dimensions of LP turbine missiles
7. Energies of LP turbine missiles

### List of Figures

1. Sectional arrangement of retrofitted LP Cylinder
- 2-16 Fault tree analysis of control and protection system
17. Panel fragment separation
18. Regions of local stress concentration
19. SCC Initiation margins for original and new rotors
20. Risk of SCC initiation below nominal threshold
21. Failure probability prediction from  $K$  and  $K_{Ic}$  distributions
22. Probability distribution for Proof Stress
23. Probability distribution for local stress
24. Probability distribution for temperature
25. Probability distribution for SCC growth rate
26. Probability of SCC initiation
27. Crack stress intensity versus crack growth at 120% speed
28. Calculated distribution of crack stress intensity
29. Probability distribution for Fracture Toughness

## 1. Introduction

This report presents the assessment of the probability of generating turbine missiles by rotor disintegration and the assessment of the characteristics of potential missiles escaping the turbine cylinders of the AEC ALSTHOM retrofitted turbine units at San Onofre. The main objective of the investigation was to demonstrate compliance with the USNRC criterion that the probability of generating missiles external to the turbine is below  $1.10^{-5}$  per unit year. Probability calculations have been based on service intervals of 10 years between rotor inspections.

As discussed in the original assessment of missile probability, there is considered to be no risk of missile generation from the HP turbine rotor or from the generator rotor because the relative masses of the stator parts are sufficient to ensure containment of any rotor fragments. The HP cylinder and generator are unchanged. In the case of the LP turbine cylinders the stator masses are much smaller in relation to the rotor masses and the possibility exists that, if a rotor were to disintegrate, external missiles could be generated, as was found to be the case for the original LP turbine. The replacement LP rotors are of different design to the originals and the internal stator parts are also different. This report addresses potential rotor fragment missiles arising from the retrofitted LP turbine.

The fundamental difference between the original and replacement rotors is that the original rotors were of shrunk-on disc construction and the replacement rotors are of welded construction as shown in Figure 1. The average level of tangential stress in the welded rotor forgings is only about 50% of that in the original discs at normal running speed. Clearly this is a major factor in improving the security of the rotors in service. The lower stress level also permits the specification of a lower Proof Stress for the rotor material, which further significantly reduces the risk of stress corrosion crack initiation and growth.

## 2. Probability of rotor fracture

### 2.1 Mechanisms of rotor fracture

Turbine missiles may be generated by disintegration of the LP turbine rotors under the following hypothetical circumstances.

- (i) If the electrical load on the turbine generator were lost and if the turbine control and protection systems then failed to prevent continuing HP steam admission then the turbine might be driven to a very high speed (runaway). The speed attained would ultimately be limited by the diminishing relative velocity of the steam and increasing losses but could reach a theoretical limit of 190% of normal speed. At this speed the level of stress in the rotor could be sufficient, without the presence of any contributory defects within the rotor, to cause ductile failure and the release of rotor fragments. Since the probability of rotor failure in this circumstance is relatively high, the probability of missile generation is of similar magnitude to the probability of the overspeed occurring.
  
- (ii) If cracks were to initiate in a rotor, by fatigue or stress corrosion, and were to extend over a period of service to a large size then there would be a risk of brittle fracture. Failure would be expected if the combination of crack size and applied stress produced a crack tip stress intensity equal to the material Fracture Toughness. If the crack size became sufficient to cause failure at the routinely applied overspeed test condition then failure would inevitably occur and the probability of failure would depend solely on the probability of the initiation and development of a crack of critical size.
  
- (iii) If cracks were to initiate by fatigue or stress corrosion but were not to develop to a size that is critical at the routinely applied overspeed test condition then they might still cause failure, but only at a higher overspeed that was not certain to occur. The probability of failure in such cases is the combined probability of both reaching the overspeed, ie the loss of electrical load and a control system failure, and of developing a crack of the corresponding critical size.

In the assessment of the probability of generating turbine missiles the probabilities of the turbine reaching specific speeds have been calculated on the basis of the probability of loss of electrical load and probabilities of failure of the control and protection system components. The probabilities of failure of the rotor at any specific speed have been calculated on the basis of the known stress levels and the probable distributions of material parameters contributing to crack initiation, crack growth and final failure.

## 2.2 Probability of attaining specific turbine overspeeds

Analysis of individual control system component faults and possible combinations of such faults enables probabilities to be assigned to each of the discrete overspeeds which might occur following accidental loss of the electrical load on the generator. These discrete overspeeds may be identified as follows,

### (a) 109 to 112% Speed

Following a full load rejection the normal action of the speed governing system will limit the maximum transient speed rise to less than 109% of normal speed. (This is less than the 110 to 111% speed setting of the emergency overspeed trip mechanisms). A speed rise to 109% will therefore occur at the same probability as that of a full load rejection.

It is recommended that in addition to regular on load testing of the overspeed trip mechanism actual overspeed trip tests are performed at twenty-four month intervals. There is therefore a probability of 1 that a speed of 112% (111% + 1% margin) occurs in each twenty-four month period.

### (b) 120% Speed (Design Overspeed)

In the event of failure of the speed governing system following a full load rejection, the speed will rise until the overspeed trip operates at nominally 110%, as described in Appendix 1, and a maximum transient rise to 120% speed will result.

### (c) 135% Speed

Failure of one or more pairs of LP emergency interceptor valves will result in the release of the energy stored in the reheater/separator. The consequence speed rise will be to approximately 135% of normal speed, as described in Appendix 1.

**(d) Runaway**

Failure of one or more pairs of HP stop and governing valves, with or without concurrent failures of pairs of LP stop and control valves, will result in continuous uncontrolled admission of steam to the turbine leading to a runaway condition of gross overspeed (up to 190% of normal speed) as described in Appendix 1.

In order to arrive at an overspeed condition of 120% speed or above it is necessary for the generator to be disconnected from the electrical distribution system as the result of an accidental disturbance when at full load. It is assumed that one full load rejection will occur once per year.

Fault trees are presented in Figures 2-16 to show possible combinations of component faults leading to loss of function resulting in uncontrolled admission of steam to the turbine. It should be noted that routes to speeds above 120% speed (Figures 6 - 16) are dependent on the specific component failures that first led to 120% speed being reached (Figures 1 - 5). Thus Figures 8 - 11 show four parallel routes to an HP line remaining open, which are then integrated in Figure 12. Figures 13 and 14 show two parallel routes to an LP line remaining open, which are then integrated in Figure 15.

No single active component fault can cause failure to trip on overspeed. Loss of power supplies is a safe condition since it leads to a trip of the unit. The failure rates used in the analysis are based on monthly on-load testing of the steam valves and the overspeed trip mechanism. Component failure rates are taken from Reference 1. The influence of test intervals is discussed in Appendix 2.

The system logic is exactly as for the original units, since the control and protection systems are unchanged. However, the numerical basis of the overall system failure probabilities has been reviewed to take account of,

- (i) The accumulation of additional relevant experience.
- (ii) The adoption of a monthly on-load test interval.
- (iii) The effect of randomness of demand to operate in the period between successive tests on the failure rates of system components per demand.

The resulting calculated probabilities of reaching specific speeds are,

Annual probability of reaching 112% speed	1.0	
Annual probability of reaching 120% speed	$2.1 \cdot 10^{-2}$	(Fig. 5)
Annual probability of reaching 135% speed	$3.0 \cdot 10^{-5}$	(Fig. 16)
Annual probability of runaway	$2.2 \cdot 10^{-6}$	(Fig. 16)

The annual probability of reaching 112% speed is, in fact, somewhat lower than 1.0, but this probability has been assumed in order to represent satisfactorily the certainty of occurrence within twenty-four months. Hence it is not necessary to consider separately the case of 109% speed.

### 2.3 Probability of LP rotor failure at specific overspeeds

#### 2.3.1 Failure at Runaway

Table 1 shows failure speeds for the LP turbine rotor calculated as the speed at which the average tangential stress reaches the failure stress, which is taken to be the average of the Proof Stress and UTS, or at which the maximum radial stress in the panel of the disc reaches the failure stress (References 2 and 3). If either of these stresses reaches the failure stress then the discs will separate into major fragments. Also shown in Table 1 are the speeds at which the blade section would fail or the root attachment would fail, at the disc bottom neck, releasing relatively minor fragments and unloading the discs. Local stresses in regions of stress concentration are not considered because they affect only small volumes of material and have an insignificant effect on ductile bursting.

In Table 1, each stage of the welded rotor is treated as a separate disc by allocation of the total hub length of each forging. Minimum and maximum failure speeds are given in columns 3 to 6, corresponding to minimum values of the tensile properties and maximum values which are 19% higher than minimum. It can be seen that failure speeds are generally above 190% of normal speed and consequently it is unlikely that ductile failure would occur even at the theoretical maximum speed (190%) to which the turbine can be driven.

Allowing for possible variation in the maximum speed at runaway and in the failure speeds of the discs, the probability of failure of an individual rotor forging has been calculated to be 0.1 or less, as discussed in Appendix 3. Allowing for the number of vulnerable forgings per unit the probability of bursting at runaway is less than 0.3, as in Appendix 3.

For those stages where the failure speeds are relatively low and failure is more likely to occur at runaway (stages 2, 3, 4 and 8), the failure speed due to radial stress is significantly lower than that due to tangential stress. Therefore, in the event of failure, it is much more likely that detachment of the disc panel would occur than disintegration of the complete forging. Detachment of a disc panel can be envisaged as initial yielding and separation along a circumferential boundary between panel and hub, followed by separation along radial lines into sectors of the panel as it stretches away from the hub as in Figure 17. Fragments of the disc panels would therefore be released, leaving the rotor hub intact.

Furthermore, as shown in columns 7 to 9 of Table 1, prior failure of root attachments or blades is likely to occur in stages 6 and 8, unloading the discs. Prior failures of this kind and the resultant disruption could cause retardation of the rotor so that no major missiles are generated.

It was concluded from a consideration of the calculated failure speeds that,

- (i) In the event of runaway the probability of rotor failure is significantly less than 1 and may be taken conservatively to be 0.3.
- (ii) Any missiles generated are likely to be sectors of detached disc panels rather than sectors of the complete forgings.

### 2.3.2 Failure at speeds below runaway

At any speed below runaway the probability of LP rotor failure was calculated by evaluating the probability distributions of,

- (a) the stress intensity of a crack that initiates and grows in the rotor over its service lifetime.
- (b) the Fracture Toughness of the rotor forging.

Rotor fragmentation is predicted when the crack stress intensity equals or exceeds the material Fracture Toughness.



### 2.3.2.1 Failure due to fatigue

Cracks may develop by fatigue or by stress corrosion during the service life of the rotors. However, growth by fatigue is limited by the very small number of stress cycles to be anticipated in service so that the maximum attainable fatigue crack size at the end of turbine life is not much larger than the initial defect size, which is itself limited to a very small size by NDT acceptance standards. Furthermore the minimum critical size of crack is large, as a result of low general stress levels and high material Fracture Toughness. In respect of both stress level and Fracture Toughness the replacement rotors are significantly better than the original shrunk-on discs, with the result that the probability of failure by fatigue crack growth from an initial defect is incalculably small. This can be illustrated by considering the most extreme and unfavourable values for all the relevant parameters, thus making it unnecessary to perform detailed probability calculations.

Calculations based on extremely conservative values for all variables and showing the safety of the rotor against fast fracture from pre-existing defects extending by fatigue are summarised in Table 2. From a consideration of the disc forging process, any significant defects are expected to be confined to the body of the rotor inside the hub diameter in regions of potential segregation. The fracture assessment has therefore been carried out assuming that a defect can occur anywhere within this region, including the positions of stress concentration at the internal radii of the inter-disc cavities and at the hub to panel fillet radii. Even if it is postulated that significant defects could occur as far out as the position of the steam pressure balance holes, analysis of defects at this position has shown that these would not be more limiting than those considered.

Within the volume of material under consideration, initial defects were considered in two different zones, differentiated according to their expected level of fracture toughness, as follows.

- (a) In the surface zone, defined as within 4 in. of the heat treated surface, the material will have experienced a rapid cooling rate during quenching and will therefore have a high toughness. An FATT of -22°F, which is the maximum allowed by the specification for test material at a depth of 4 in. from the heat treated surface of these discs, has been assumed for material within this zone (Reference 3).

- (b) In the sub-surface zone, defined as more than 4 in. from a heat treated surface, the material will have been subjected to a lower rate of cooling during quenching. There will therefore be a gradual reduction of toughness with depth below the surface zone, with the lowest toughness occurring at the centre of the disc. For material in the sub-surface zone an FATT of +95°F, which is equal to the maximum allowed by the specification if test material were taken from the centre of bored forgings, has been pessimistically assumed. (Note, however, that the forgings for the San Onofre rotors will not be bored).

The minimum toughness for material in each zone has been taken to be 90% of the value obtained from the lower bound correlation between Fracture Toughness and excess temperature (Temperature minus FATT) for NiCrMo rotor steel, as obtained from Reference 4.

The effective stress range for the most critical location in each of these zones due to a start-up/shut-down cycle has been established by examination of the Finite Element stress analysis results (Ref. 5). Centrifugal stresses have been combined with transient thermal stresses, assuming partial effectiveness of the contribution of compressive stresses to crack growth, to give the effective stress ranges shown in Table 2. The highest stresses occur at the rotor surface due to local stress concentrations.

For both zones, the maximum indication permitted by the ultrasonic inspection standard is 0.12 in. Flat Bottom Hole equivalent diameter. For the purpose of this analysis it was very conservatively assumed that an ultrasonic indication of twice the maximum permitted size exists, and corresponds to an actual defect which is twice the FBH equivalent size, ie. 0.48 in. actual defect diameter. In the case of the surface zone it was assumed that the defect lies just below the finish machined surface of the rotor, and on first loading breaks through to become a semicircular surface defect with radius 0.48 in. In both cases it was assumed that these defects are sharp cracks situated at the position of maximum stress and are subjected to a uniform normal stress equal to the maximum quoted value. No account was taken of the decay in stress away from the peak surface value.

These postulated initial defects were assumed to extend in service under repeated centrifugal and thermal stress cycles, due to turbine starting, at a rate which was very conservatively taken to be twice the upper bound of growth rate data for NiCrMo rotor steel. The calculated maximum fatigue extended defect sizes at the end of a service life of 500 starts, all of which were assumed to include an overspeed test to 112%

normal speed, are given in Table 2. It can be seen that little fatigue crack growth was calculated to occur within the service life of the rotors.

Also shown in Table 2 are the calculated minimum critical defect sizes for fast fracture under the conditions of an overspeed to 120% normal speed at a temperature of 68°F. These conditions are far more severe than any which might reasonably be expected to occur in service. The total stress at the overspeed event includes conservative allowances for thermal and residual stresses.

It can be seen that the ratio of minimum critical defect size to maximum fatigue extended defect size is 2.8 for the surface zone, and greater than 5 for the sub-surface zone. Therefore, even with the compounded effect of repeatedly conservative assumptions, the calculated margins of safety against fast fracture at the end of life are large and the probability of fracture from a fatigue extended defect is clearly negligible.

#### 2.3.2.2 Failure due to stress corrosion

Peak rotor stresses in regions of stress concentration are shown in Table 3 together with the threshold stress for stress corrosion cracking corresponding to the local temperature (see Reference 6). The locations of these regions of stress concentration are shown in Figure 18. It can be seen that peak stresses in the rotors are lower than the expected threshold for crack initiation, and therefore cracking should never occur. Figure 19 shows the peak stresses and Proof Stress range for the original stage 4 discs relative to the nominal threshold, where stress corrosion cracking occurred in service at the balance holes and straddle root fillets. Also shown are the peak stresses at the root attachment pin-holes, at the balance holes and at the panel fillets for the new rotors, together with the lower Proof Stress range, demonstrating the great improvement that has been made.

However, a conservative statistical analysis of the available laboratory data (Reference 7) has been performed which allows for the possibility of initiation at conditions below the nominal threshold at low levels of probability. This is illustrated by Figure 20, in which the 95% confidence level of no crack initiation corresponds to the nominal threshold. It is this conservative model that has been used for the calculation of failure probability.

In order to calculate the probability of failure of the new rotors due to SCC, a Monte Carlo analysis was performed to determine the probable distribution of crack stress

intensity for an extended crack in service prior to inspection. This was then combined with the probable distribution of material Fracture Toughness to obtain the probability of fracture, as indicated schematically in Figure 21. For the Monte Carlo analysis of stress intensity a large number of trial calculations (ten million) was carried out and in each trial the values of each of the following variable parameters was randomly selected from a pre-determined probability distribution. The basis of the individual parameter distributions is shown in the corresponding figures.

- (i) Material Proof Stress (see Figure 22)
- (ii) Maximum local stress (see Figure 23)
- (iii) Temperature (see Figure 24)
- (iv) Crack growth rate (see Figure 25), from Reference 8

In addition, the probability of SCC initiation was calculated from the input variables as in Figure 26, corresponding to Figure 20.

The calculations were performed for the specific case of a stage 4 disc which, by reason of being the first fully wet disc and having a lower margin than any other fully wet disc relative to the nominal SCC threshold, must have the highest probability of any disc of failure from SCC. It was assumed that cracks would extend over ten-year periods of virtually continuous service to obtain the final crack size that could exist just prior to inspection. It was assumed that there was no incubation period prior to crack initiation, which is very conservative as regards the first ten-year period of operation and is more realistic for a second or subsequent period of operation.

Depending on the assumed location of the crack and its calculated extension, the calculated crack size was increased to incorporate the attachment pin-hole diameter or balance hole diameter (or both) intersected by the crack. Account was also taken of the possible coalescence of independently initiating cracks as indicated in Figure 27. Separate analysis was carried out for cracks initiating at an attachment pin-hole or at both balance hole and pin-hole or at the fillet radius between disc panel and rotor hub. The stress intensity for each crack was calculated from its final size and the nominal stresses in the rotor at any selected overspeed. Table 4 presents the results of two illustrative examples of trial calculation.

An example of the resultant calculated distribution of crack stress intensity is shown in Figure 28. The changes in gradient of this curve are directly related to changes in gradient in the stress intensity versus crack size curve of Figure 27.

Finally, the probable distribution of material Fracture Toughness, as defined in Figure 29, was combined with the calculated stress intensities to obtain a probability of failure as illustrated in Figure 21. A somewhat simpler procedure was adopted for fillet cracks, since the extension of cracks from opposite sides leaves a ligament between the two which fails under direct stress before the stress intensity approaches the Fracture Toughness. Failure probabilities were added for the different crack origins considered to obtain the total probability of a stage 4 disc failing, conditional on the selected overspeed being reached. Table 5 shows the summation of these probabilities at overspeeds of interest.

The figures in Table 5 were generated by analysis of a single stage 4 disc. There are three stage 4 discs per unit, plus three stage 3 discs at a similar level of risk, six stage 5 discs at a lower level of risk and other stages at a relatively insignificant level of risk (see Table 2). The probability of failure per unit was equated to the probability of failure of ten stage 4 discs, as below.

St. 4 discs	St. 3 discs	St. 5 discs	Others	Total
$3 \times P_4$	$+ 3 \times P_4$	$+ 6 \times 0.5 P_4$	$+ P_4$	$= 10 \times P_4$

The resultant probabilities of failure per unit at specific speeds, conditional on reaching those speeds and strictly valid at the end of ten years if no prior overspeeds have occurred, were then obtained as follows.

Unit conditional probability of SCC failure	at 112% speed = $2.8 \cdot 10^{-6}$
	at 120% speed = $1.1 \cdot 10^{-5}$
	at 135% speed = $3.9 \cdot 10^{-5}$

Failure probabilities at each speed are inclusive of failure probabilities at any lower speed. For example, the probability of failure at 120% speed having survived at 112% speed is  $1.1 \cdot 10^{-5} - 2.8 \cdot 10^{-6} = 8.2 \cdot 10^{-6}$ .

#### 2.4 Overall probabilities of failure

For low overspeed failures (112% to 135% normal speed), the SCC failure mechanism governs. This mechanism is progressive and the risk of failure increases as cracks extend with time in service between inspections. It is necessary to establish the

maximum annual probability of failure at any chosen speed and this must occur in the year prior to inspection, i.e. in the tenth (or twentieth, or thirtieth) year of operation. The probability of failure in this year is considerably higher than the average, but is lower than the value given in the previous section because of the probability of failure in previous years within the inspection cycle. In the case of 112% speed, which is assumed to occur once per year, the probability of failure in the tenth year is the probability of failure at the end of ten years, as in the previous section, minus the probability of failure at the end of nine years. The probability of failure in the tenth year has thus been determined to be  $2.8 \cdot 10^{-6} - 1.9 \cdot 10^{-6} = 9.0 \cdot 10^{-7}$ . This effect may be neglected for overspeeds of 120% and 135% because the probabilities of prior occurrence of the overspeeds are relatively small. For runaway overspeed the failure mechanism is not progressive and the conditional failure probability remains constant with time.

The overall maximum probability of failure at any speed is the simple product of the probability of reaching that speed and the conditional probability of failing at that speed, corrected to exclude prior failures in earlier years or at lower speeds. The overall probabilities of failure were thus obtained as follows.

(i) Annual probability of failure at 112% speed,

$$\begin{aligned} \text{Annual probability of reaching 112\% speed} &= 1.0 \\ \text{Probability of failing at 112\% speed} &= 2.8 \cdot 10^{-6} \\ \text{Max. annual probability of failure at 112\% speed} &= 1.0 \times (2.8 \cdot 10^{-6} - 1.9 \cdot 10^{-6}) \\ &= 9.0 \cdot 10^{-7} \end{aligned}$$

(ii) Annual probability of failure at 120% speed,

$$\begin{aligned} \text{Annual probability of reaching 120\% speed} &= 2.1 \cdot 10^{-2} \\ \text{Probability of failing at 120\% speed} &= 1.1 \cdot 10^{-5} \\ \text{Max. annual probability of failure at 120\% speed} &= 2.1 \cdot 10^{-2} \times (1.1 \cdot 10^{-5} - 2.8 \cdot 10^{-6}) \\ &= 1.7 \cdot 10^{-7} \end{aligned}$$

(iii) Annual probability of failure at 135% speed,

$$\begin{aligned} \text{Annual probability of reaching 135\% speed} &= 3.0 \cdot 10^{-5} \\ \text{Probability of failure at 135\% speed} &= 3.9 \cdot 10^{-5} \\ \text{Max. annual probability of failure at 135\% speed} &= 3.0 \cdot 10^{-5} \times (3.9 \cdot 10^{-5} - 1.1 \cdot 10^{-5}) \\ &= 8.4 \cdot 10^{-10} \end{aligned}$$

(iv) Annual probability of failure at runaway,

Annual probability of reaching runaway speed	= $2.2 \cdot 10^{-6}$
Probability of failure at runaway speed	= 0.3
Annual probability of failure at runaway	= $2.2 \cdot 10^{-6} \times (0.3 - 3.9 \cdot 10^{-5})$
	= $6.6 \cdot 10^{-7}$
Total annual probability of failure (at any speed)	= $1.7 \cdot 10^{-6}$

It is apparent that the probability of a rotor reaching runaway speed and disintegrating is of similar magnitude to the probability of disintegrating at lower overspeeds due to the development of a stress corrosion crack.

The annual probability of failure, i.e. the annual probability that a rotor will disintegrate and release major fragments within any one unit, is significantly lower than the required limit of  $1 \cdot 10^{-5}$  for external missiles. Hence this criterion is satisfied irrespective of whether the rotor fragments are capable of penetrating the surrounding casings. Nonetheless an analysis has been performed of the masses and energies of potential missiles and of the losses in energy likely to be encountered in casing penetration.

### 3. Turbine missile characteristics

#### 3.1 Mechanism of disintegration

The figures presented in the preceding section show that there is a fairly similar probability of missile generation at low overspeeds and at runaway overspeed. As discussed in section 2.3.1, in the event of bursting at runaway the disc panels can be expected to separate from the central hub portions of the rotor forgings, releasing disc panel fragments as sketched in Figure 17. The largest and most energetic potential missiles at runaway are fragments of a stage 8 disc.

In the event of a low speed burst, caused by the development of a stress corrosion crack of critical size, the manner of disintegration will depend upon the origin of the crack and its direction of extension. If cracks were to originate at the panel to hub fillet radius they would be likely to extend across the base of the panel, separating the panel from the hub and leading to the release of panel fragments. In the case of cracks originating at the pin holes and/or balance holes and extending in a radial direction,

it is possible that eventual fast fracture could propagate, in an axial-radial plane, across an entire forging. For example, if a stress corrosion crack were to form at the pin or balance holes in a Stage 4 disc, where the risk is greatest, rotor fragments might be released which are complete sectors of the Stage 1-4 forging.

Bearing in mind the above limitations to the kind of rotor fragments which might be released internal to the turbine, missile analysis has been carried out for the following specific fragment types.

- (a) Sectors of a Stage 4 disc panel at 120% speed.
- (b) Sectors of a Stage 1-4 rotor forging at 120% speed.
- (c) Sectors of a Stage 4 disc panel at 190% speed.
- (d) Sectors of a Stage 8 disc at 190% speed.

For the Stage 8 disc, the difference between the bursting speeds calculated from the radial stress and the tangential stress is small (see Table 1), and the difference in energy between a panel fragment and a complete panel plus hub fragment is small. Therefore fragments have been considered which incorporate both panel and hub.

### 3.2 Size of missiles

As for the analysis of the original rotors, a number of simplifying assumptions were made concerning the nature of the rotor fragments, as follows.

- (i) It was assumed that disintegrating disc panels or rotor forgings break into four 90° sectors. It is just as likely that three equal 120° sectors or five equal 72° sectors, or unequal fragments within this size range might be released. However, previous calculations have shown that fragments larger than 90°, although having greater mass and energy, are no more likely to penetrate the surrounding casings. This is because larger fragments have less translational kinetic energy per unit mass and present a greater area of impact to any barrier. A 90° quadrant is therefore satisfactorily representative of the worst likely missile.
- (ii) It was assumed that the rotational component of fragment initial kinetic energy is dissipated in friction and scraping during impact with the stationary parts. Calculations of fragment energy lost in impact were therefore based entirely on its initial translational kinetic energy. Obviously if a missile were to escape the



casings with a significant proportion of its initial translational k.e. remaining it could reasonably be supposed that it retains a similar proportion of its initial rotational k.e.

- (iii) Blading initially attached to any rotor fragment was assumed to be broken off and scattered during impact with the surrounding casing parts. Blade root attachments were assumed to remain integral with the rotor fragment.

The sizes and masses of the rotor fragments considered are detailed in Table 6. Comparing the specific fragment types considered to the shrunk-on disc fragments considered for the original rotors, the following differences are noted. The Stage 4 panel fragment is small, being only about one quarter of the axial width and one third to one quarter of the original disc fragment masses. The Stage 8 hub fragment is of similar dimensions and mass to the original disc fragments. The Stage 1-4 forging fragment is twice the axial length and about twice the mass of the original disc fragments.

### 3.3 Energy lost in casing penetration

Fragments released by rotor disintegration are obstructed by the surrounding stationary parts, including the diaphragms, the diaphragm carriers, the inner casing parts and the outer casing as shown in Figure 1. Compared to the original structure the retrofitted casing presents a somewhat greater resistance to penetration because the diaphragm rings are cast steel instead of cast iron and the exhaust diffuser is of heavier construction. The basis for assessing the energy lost by a rotor fragment in penetrating these structures was the same in principle as for the analysis of the original shrunk-on disc fragments and is summarised below.

- (i) A fragment impacting on a stationary structure was assumed to enter into an inelastic collision which, if completed (see below), resulted in a net energy loss and in the displaced obstacle being carried forward with the disc fragment at a common velocity. The volume of the obstacle involved at each impact included a 90° circumferential arc, corresponding to each of four rotor fragments, and an axial extent in line with the rotor fragment.

Diaphragm rings, which have insufficient bolting to be considered continuous at the joint, were treated as free bodies undergoing inelastic collision only.

- (ii) The energy required to perforate the obstacle by a combination of shear around the impact periphery and compression over the impact area was calculated. If this was less than the inelastic collision loss then perforation was assumed to occur before the whole of the obstacle could be accelerated forward. The energy loss was then only the lesser amount due to shear and compression. A part of the obstacle in the direct path of the missile was assumed carried forward with the incident missile at a common velocity. If sufficient space separated this impact from the next impact then the displaced mass of the first obstacle was assumed scattered before impacting the next. Otherwise the displaced mass was assumed to remain part of a composite missile at the next impact.
  
- (iii) If perforation did not occur then the whole of the barrier was assumed to be accelerated outward and the energy required to rupture the barrier by stretching over its whole volume was calculated. If this was less than the energy of the incident missile (and any debris displaced from earlier impacts, including any subsequently scattered) then the barrier was assumed to fail by stretching. The stretching energy was deducted from the incident missile energy and a part of the barrier in the direct path of the incident missile was assumed carried forward at a common velocity.
  
- (iv) If perforation did not occur and the missile (plus debris) energy was insufficient to fail the obstacle by stretching then the missile was assumed to be contained.

The results of applying this method of analysis to specific rotor fragments are shown in Table 7. For missiles released at 120% of normal speed, the Stage 4 panel fragment was calculated to escape the casings with less than 20% of its initial energy and the relatively large Stage 1-4 forging fragment was calculated to be contained. The larger fragment was contained because it impacts with the whole mass of the trapped diaphragms and encounters a proportionally higher resistance within the inner casing. The results are consistent with those for the original shrunk-on discs which showed that fragments of Stages 1-5 discs released at 120% speed would be contained.

For missiles released at 190% of normal speed, both the Stage 4 and Stage 8 fragments were calculated to escape the casings. The Stage 8 fragment has considerably greater mass and escape energy and retains about one third of its initial energy. The Stage 8 missile, which is the most massive and energetic external missile

considered, has a mass (5520 lbn) and an energy ( $16.1 \cdot 10^6$  ft lbf) lower than those of the most massive and energetic missile of the original rotor (6500 lbn,  $27.1 \cdot 10^6$  ft lbf).

4. Probability of generating external missiles

It has been shown in section 2.4 that the annual probability of rotor failure is roughly equally attributable to the probability of failure at runaway and the probability of failure at low overspeeds. Consideration of the type of rotor fragments likely to be released at runaway, as in the preceding section, shows that such fragments are likely to penetrate the surrounding casings and become external missiles. The annual probability of generating external missiles at runaway is therefore numerically the same as the annual probability of rotor failure at runaway, i.e.  $6.6 \cdot 10^{-7}$ .

The annual probability of failure at low overspeeds is  $1.1 \cdot 10^{-6}$ . Consideration of the type of rotor fragments likely to be released at low overspeeds shows that such fragments may become external missiles with relatively low energies or may be contained. The probability of rotor fragments becoming external missiles at low overspeed is therefore somewhat lower than .1, but this is of little consequence in the context of the overall probability of generating external missiles at any speed. The total annual probability of generating external missiles may therefore conservatively be assumed equal to the total annual probability of failure, which is  $1.7 \cdot 10^{-6}$  per unit. This is well within the USNRC target of  $1 \cdot 10^{-5}$  per unit year.

APPENDIX 1 : OVERSPEED ANALYSIS

1. Design overspeed (120% speed)

For determination of the maximum design overspeed the following extreme sequence has been assumed,

- (i) The turbine is operating at full load with all turbine valves wide open.
- (ii) The entire turbine load is rejected instantaneously (no allowance is made for unit auxiliary load).
- (iii) The turbine speed control system fails to respond (no attempt is made to control speed rise).
- (iv) A trip is initiated at the maximum set point of the duplicate overspeed trips (110% + 1% speed).
- (v) Subsequently the turbine valves operate in the manner described below.

At the instant of the load rejection the turbine is assumed to accelerate at a constant maximum rate corresponding to the torque produced by the full load steam flow and the rotational inertia of the unit until it reaches the maximum overspeed trip setting of 111%. A time delay of 0.08 secs. is allowed for before the steam admission valves start to close. Further flow into the turbine during valve closure is then calculated on the basis of valve flow area during closing. The closing time for all HP stop and control valves beyond the 0.08 secs. delay is 0.26 secs. and for all LP stop and control valves is 1.2 secs. beyond the 0.08 secs. delay.

The additional overspeed is then calculated using the energy of the steam entering the machine during valve closure and the energy of the stored steam and water within the relevant parts of the turbine and interconnecting pipes. The resulting maximum overspeed calculated for the machine is 120% of synchronous speed.

Valve closure times as above are based on current limits observed at SONGS. The overspeed reached is fairly insensitive to valve closure times. For example, a 20% increase in both HP and LP valve closure times produces an increase in overspeed of only 0.6% of normal speed.

2. 135% speed

Following the same sequence as for design overspeed up to overspeed trip operation at 111% speed, the HP valves are assumed to close but malfunction of the LP valves results in continued steam admission from the reheater/separator. The additional steam energy results in a higher overspeed.

3. Runaway overspeed

The runaway speed attainable is fundamentally dependent on the steam speed to blade speed ratio. Acceleration of the rotor line to the point that the steam has zero relative velocity imposes an upper limit on the runaway speed. For a design speed ratio of 2, i.e.  $U/C_0 = 0.5$  as for the San Onofre turbine, the notional runaway overspeed is 200% of normal speed and a small allowance for increased losses reduces this to 190%.

Note, however, that allowance has been made in assessing the probability of failure for a variation in runaway speed up to 210% of normal speed (see Appendix 3).

APPENDIX 2 : INFLUENCE OF TEST INTERVALS ON FAILURE PROBABILITY

Component failure rates increase exponentially with test interval. However, for low failure rates (i.e. much less than 1, as for all components of the control and protection system in Figures 2 - 16) this is equivalent to a linear increase with test interval. The effect of increasing test intervals may be examined by increasing the failure rates per demand of the relevant components in direct proportion, and following the logic of Figures 2 - 16 to obtain the increased overspeed probabilities. The only modification to the fault tree logic is that, where a common analysis is given in Figures 2 and 7 for both HP and LP valve hydraulic actuators tested at a common frequency, a difference in test frequencies for HP and LP valve actuators will lead to a difference in failure rates.

Taking these effects into account, the result of increasing the LP valve on-load test interval and the overspeed trip test interval is shown in the table below. Case A is the base case discussed in this report

Case	A (Base)	B	C	D
OLT interval (months) : HP valves	1	1	1	1
LP valves	1	3	3	6
O/S trip	1	1	3	3
Annual O/S probabilities:				
112%	1.0	1.0	1.0	1.0
120%	$2.1 \cdot 10^{-2}$	$3.9 \cdot 10^{-2}$	$3.9 \cdot 10^{-2}$	$6.6 \cdot 10^{-2}$
135%	$3.0 \cdot 10^{-5}$	$2.6 \cdot 10^{-4}$	$2.6 \cdot 10^{-4}$	$1.1 \cdot 10^{-3}$
Runaway	$2.2 \cdot 10^{-6}$	$2.2 \cdot 10^{-6}$	$2.2 \cdot 10^{-6}$	$2.2 \cdot 10^{-6}$

The probabilities of reaching 112% speed and runaway are unaffected by any of these changes. The probabilities of reaching 120% and 135% speed are affected by increases in the LP valve OLT interval but are affected only to a negligible extent by increase in the overspeed trip test interval.

The annual probabilities of rotor failure, calculated as in section 2.4 of this report, then become,

Case	A (Base)	B	C	D
Annual failure probabilities:				
112%	$9.0 \cdot 10^{-7}$	$9.0 \cdot 10^{-7}$	$9.0 \cdot 10^{-7}$	$9.0 \cdot 10^{-7}$
120%	$1.7 \cdot 10^{-7}$	$3.2 \cdot 10^{-7}$	$3.2 \cdot 10^{-7}$	$5.3 \cdot 10^{-7}$
135%	$8.4 \cdot 10^{-10}$	$7.3 \cdot 10^{-9}$	$7.3 \cdot 10^{-9}$	$3.1 \cdot 10^{-8}$
Runaway	$6.6 \cdot 10^{-7}$	$6.6 \cdot 10^{-7}$	$6.6 \cdot 10^{-7}$	$6.6 \cdot 10^{-7}$
Total	$1.7 \cdot 10^{-6}$	$1.9 \cdot 10^{-6}$	$1.9 \cdot 10^{-6}$	$2.1 \cdot 10^{-6}$

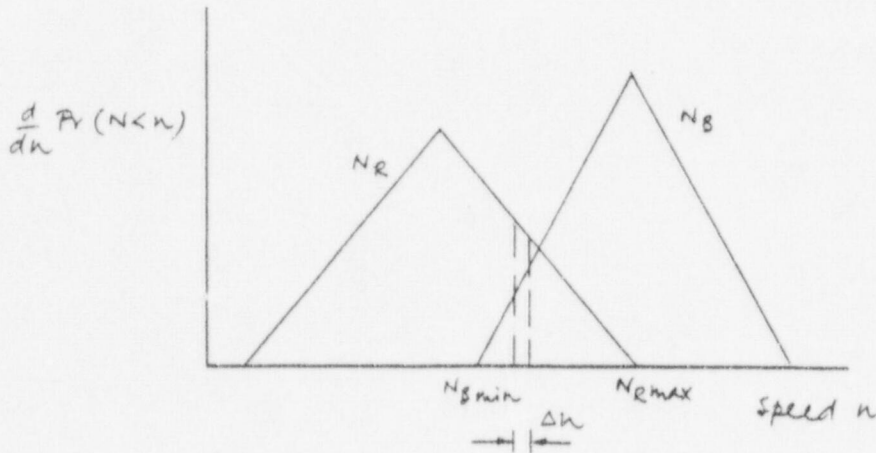
The failure probabilities are scarcely altered by the increases in test intervals considered. This is because the only overspeed probabilities that increase significantly, at 120% and 135% speed, contributed little to the total failure probability in the base case.

APPENDIX 3 : PROBABILITY OF BURSTING AT RUNAWAY OVERSPEED

The nominal value of runaway overspeed is lower than the calculated minimum bursting speeds for separation of the rotor forgings into major fragments, as shown in Table 1. This implies zero risk of bursting speed at runaway. Allowance has been made for variation in both runaway overspeed and bursting speeds in order to derive a representative failure probability.

The runaway overspeed ( $N_R$ ), which is nominally 190% of normal speed, has been assumed to lie between 180% and 210% of normal speed with a conservative mean value of 195% and a symmetrical linear probability density as in the diagram below. Bursting speeds ( $N_B$ ) have been assumed to lie within the range of the worst stage in each forging as follows, with a symmetrical linear probability density as in the diagram.

Stage 1 - 4 forging	196% - 213% )
Stage 5 - 7 forging	211% - 230% ) from Table 1
Stage 8 forging	205% - 223% )



Probabilities of failure in the overlap region of these probability densities were calculated by integrating the probability of a runaway speed in the small interval  $\Delta n$  and a bursting speed below the middle of that interval. Expressed algebraically the integration is,

$$\sum_{n = N_{Bmin}}^{n = N_{Bmax}} \Pr \left( n - \frac{\Delta n}{2} < N_R < n + \frac{\Delta n}{2} \right) \times \Pr (N_B < n)$$



The resultant failure probabilities are,	Stage 1 - 4 forging	0.095
	Stage 5 - 7 forging	0
	Stage 8 forging	0.002

Taking account of the number of forgings of each kind present in one unit (three St. 1 - 4, six St. 5 - 7 and six St. 8 forgings) the overall probability of bursting at the runaway condition is,

$$1 - (1-0.095)^3 (1-0.002)^6 (1-0)^6 = 0.27$$

The slightly more conservative value of 0.3 has been used in the calculation of overall failure probability.

APPENDIX 4 : REFERENCE SOURCES

Information utilised in developing the analysis presented in this report was taken from the following reference sources.

1. Failure rates for control and protection system components from published generic data for similar components (conservatively de-rated) and internal records of service performance.
2. GEC ALSTHOM standard rotor centrifugal stress calculations (using quality assured internal computer program DISTRESS 1.3).
3. Mechanical properties in accordance with specification SBV MF 1023 Issue E (with amendment 754 G 90574A) and design data norms showing the effect of temperature.
4. GEC ALSTHOM data and published data correlation between measured Fracture Toughness and excess temperature (test temp. minus FATT) for NiCrMo and NiCrMoV rotor forgings.
5. Technical submission No.10, LP rotor stress analysis.
6. Technical submission No.39, LP rotor stress corrosion design margins.
7. GEC ALSTHOM laboratory data on SCC initiation in long term tests (see also Ref.6 and GEC ALSTHOM document "Stress corrosion research and industrial experience on NiCrMoV rotor steels", 11th June 1996.
8. GEC ALSTHOM data and published data on stress corrosion crack sizes observed in service and rates of growth observed from service and laboratory tests (as in GEC ALSTHOM document TM 95/015).

Forging	Stage	Bursting speed (% of normal speed)						
		Average disc hoop stress		Max. disc panel radial stress		Disc bottom neck stress		Max. blade stress
		Min.	Max.	Min.	Max.	Min.	Max.	Max.
Stages 1-4	1	262	285	219	238	263	286	340
	2	260	293	196	213	220	240	308
	3	250	272	200	218	239	260	304
	4	219	238	202	220	232	252	272
Stages 5-7	5	220	239	218	238	212	231	316
	6	240	262	211	230	185	201	264
	7	228	248	233	253	220	240	282
Stage 8	8	212	231	205	223	176	191	185

Notes:

1. Minimum disc failure speeds are calculated for minimum tensile properties (average of Proof Stress and UTS). Maximum disc failure speeds are calculated for tensile properties 19% higher than minimum.
2. Rotor disintegration into major fragments will occur if the average disc hoop stress or maximum disc panel radial stress reach the failure stress. Prior failure within the blade or the root attachment (disc bottom neck) will release relatively minor fragments and unload the rotor.

**Table 1. Calculated bursting speeds of San Onofre rotor forgings**

**Table 2. Fatigue crack growth calculations**

	Zone	
	Surface ( < 4" from heat treated surface)	Sub Surface ( > 4" from heat treated surface)
Effective stress range for cycle (ksi)	70.4	36.3
Max. permitted indication FBH diameter (in)	0.12	0.12
Assumed indication FBH diameter (in)	0.24	0.24
Assumed initial defect radius (in)	0.48	0.24
Maximum calculated fatigue extended defect radius (in)	0.59	0.24
Max. FATT (°F)	-22	+95
Critical event: Cold overspeed to 120%		
Temperature (°F)	68	68
Min. fracture toughness* (ksi√in)	135	72
Max. total stress at critical event (ksi)	83.3	56.3
Min. critical crack radius (in)	1.65	1.29
<u>Min. critical crack radius</u>		
Max. extended crack rad.	2.8	5.4

\* Very conservative values of fracture toughness have been used relative to expected values.

## AFFIDAVIT

In the town of Rugby

and County of Warwickshire, England

I, Gary Furnival being duly sworn, hereby say and depose:

1. I am Project Manager with responsibility for the LP Turbine Retrofit of San Onofre Nuclear Generating Station for ALSTOM Energy Ltd (hereinafter referred to as ALSTOM) of Newbold Road, Rugby, Warwickshire, England.
2. I have read ALSTOM's reports entitled "San Onofre 2&3 - Replacement LP Rotors" dated 17<sup>th</sup> of September 1998 and "San Onofre Missile Analysis" hereinafter referred to as the Documents.
3. The Documents contain information of a proprietary and commercially sensitive nature which is regarded as strictly confidential by ALSTOM and shall not be released into the public domain. To the best of my knowledge and belief ALSTOM's competitor companies regard information of the kind contained in the Documents as proprietary and confidential.
4. We have made the Documents available, in confidence, to the US Nuclear Regulatory Commission, at the request of our customer Southern California Edison, with the request that the information contained in the Documents shall not be disclosed or divulged to third parties.
5. The information contained in the Documents reveals important aspects of ALSTOM's steam turbine design which has been developed through many years of extensive research and development activity giving ALSTOM steam turbines crucial enhancements over competitor's equipment sufficient to enable ALSTOM to maintain a

technical and commercial advantage over those of its competitors who are not in possession of the information contained in the Documents.

6. The disclosure of the proprietary information contained in the Documents to a competitor, not in possession of the information contained in the Documents, would result in substantial harm to the commercial interests of ALSTOM.
7. Information contained in the Documents has been made available, on a limited basis, to others outside of ALSTOM, only in accordance with strict conditions of confidentiality permitting its use for defined purposes and providing for nondisclosure to third parties.
8. ALSTOM require that such proprietary information released by ALSTOM to others should be kept in a secure file and not disclosed to third parties without the written consent of ALSTOM.

I hereby declare that the statements made hereinabove are, to the best of my knowledge, information and belief, truthful and complete

Signed

Gary Hunt

*SWORD*

SIGNED before me

this *18th* Day of *September* 1998  
at *16, Church Street*  
*Rugby*

BRETHERTONS  
16 CHURCH STREET  
RUGBY  
WARCS. CV21 3PW

*Paul Smith*  
(PAUL SMITH)

BRETHERTONS  
COMMISSIONERS FOR OATHS

*A Commissioner for Oaths*

ENCLOSURE 4

RELEASE OF COPYRIGHTED MATERIAL

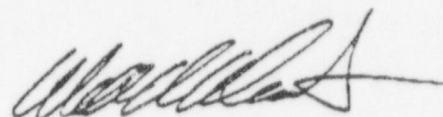
# ALSTOM

## ENERGY

Service & Retrofit

### CONTRACT NO. 8G076001: MAIN TURBINE LOW PRESSURE ROTOR SETS FOR SAN ONOFRE NUCLEAR GENERATING STATION: MISSILE ANALYSIS REPORT

"In furtherance of the requirements of Section 3.7.3 of the above Contract, ALSTOM USA Inc. hereby agrees, on behalf of the ALSTOM Group of Companies, that the NRC may make such additional copies of the figures included in report "San Onofre 2 & 3 Replacement L.P Rotors reference SONGSA1101" dated September 17, 1998 prepared by ALSTOM and submitted to Southern California Edison on September 17, 1998 in accordance with the aforesaid Section as may be necessary to enable the NRC to consider the contents of the said Report, notwithstanding the copyright statement of GEC ALSTHOM thereon. Such additional copies of the said Report made by the NRC shall be for the internal use of the NRC only and shall not made part of any public record."



William F. Van Wart  
General Manager  
ENERGY  
Service & Retrofit